Small polaron hopping conduction and magnetic frustration in the electron-doped charge ordered $Ca_{0.85}La_{0.15}MnO_3$ system



2007 J. Phys.: Condens. Matter 19 486201

(http://iopscience.iop.org/0953-8984/19/48/486201)

IOP PUBLISHING JOURNAL OF PHYSICS: CONDENSED MATTER

J. Phys.: Condens. Matter **19** (2007) 486201 (8pp) doi:10.1088/0953-8984/19/48/486201

# Small polaron hopping conduction and magnetic frustration in the electron-doped charge ordered $Ca_{0.85}La_{0.15}MnO_3$ system

**Esa Bose, S Karmakar and B K Chaudhuri**[1]

Department of Solid State Physics, Indian Association for the Cultivation of Science, Kolkata-700032, India

E-mail: sspbkc@iacs.res.in

Received 16 July 2007, in final form 12 October 2007
Published 6 November 2007
Online at stacks.iop.org/JPhysCM/19/486201

**Abstract**

The electron-doped $Ca_{0.85}La_{0.15}MnO_3$ system exhibits a charge ordering transition at ∼135 K ($T_{CO}$) with the antiferromagnetic Néel temperature at 160 K ($T_N$). The resistivity data above and below $T_N$ (down to 90 K) are found to follow the small polaron hopping conduction mechanism. The corresponding activation energy, estimated from the theoretical fitting of resistivity data, shows an anomalous increase below $T_N$, supporting the aforementioned charge ordering phenomenon. This result is further confirmed from fitting of the current–voltage ($I$–$V$) data with the small polaron hopping model. As revealed from the field cooled and zero field cooled magnetization measurements, this electron-doped system exhibits the signature of magnetic frustration, below $T_{CO}$ associated with phase separation behavior.

(Some figures in this article are in colour only in the electronic version)

## 1. Introduction

After the discovery of the colossal magnetoresistive (CMR) property in $La_{1-x}Ba_xMnO_3$ [1] in 1993, manganites with perovskite structure have widely been investigated. The basic transport mechanism in such oxides has been explained considering double-exchange (DE) interaction together with the Jahn–Teller (JT) effect [2, 3]. Most of the earlier studies were, however, concentrated on the hole-doped manganites $L_{1-x}A_xMnO_3$ ($x < 0.5$) [4–8], where L is a lanthanide and A is an alkaline-earth cation, while the electron-doped manganites which correspond to $Mn^{4+}$-rich compounds have not been extensively studied, as they do not exhibit CMR effects [9–11]. Recent discovery of new ferromagnetic (FM) metallic manganites, namely $Ca_{1-x}L_xMnO_3$ and $Ca_{1-x}Bi_xMnO_3$ ($x \sim 0.10$) [12, 13], has attracted much attention

[1] Author to whom any correspondence should be addressed.

  

because it suggests the possibility of exhibiting magnetoresistance in electron-doped systems. Unlike the hole-doped manganites, the CMR effect in electron-doped manganites has, however, been observed only in a narrow region of the phase diagram. For example, $Ca_{1-x}L_xMnO_3$ ($x < 0.5$) exhibits the CMR effect at around the critical concentration $x_c$ (∼0.8–0.9) [12, 14]. Charge ordering phenomena together with an antiferromagnetic (AF) ordering state are observed for $x < x_c$, while a ferromagnetic metallic state appears for $x > x_c$. The competing behavior existing among charge ordering, AF ordering and the ferromagnetic metallicity leads to the CMR effect at the phase boundary of $x = x_c$.

However, little emphasis has so far been placed on the transport mechanism of the low electron doping region of the Ca(La)$MnO_3$ system. Our plan in the present study is to address this point in a typical sample prepared by adding a low electron concentration (15%) to $CaMnO_3$ through substitution of $La^{3+}$ for $Ca^{2+}$. $CaMnO_3$, being less prone to chemical defects than $LaMnO_3$ [15], is an ideal system for detailed studies in the low electron doping regime. Interestingly, small polaron hopping conduction was observed in this system till low temperatures of about 90 K. This result was deduced from the resistivity and $I$–$V$ measurements. Temperature dependent field cooled (FC) and zero field cooled (ZFC) magnetization measurements were performed, revealing the presence of magnetic frustration in the compound.

## 2. Experimental details

A polycrystalline sample, $Ca_{0.85}La_{0.15}MnO_3$, was prepared by using a standard solid state reaction method. The precursors CaO, $La_2O_3$ and $MnO_2$ (each of purity better than 99.9%) were mixed in proper stoichiometric composition, ground and then preheated at 1173 K for 24 h. The mixed powders thus obtained were reground, pelletized (bar shaped) and sintered at 1523 K for 12 h. The same procedure was repeated once more and finally the pellets were sintered at 1773 K for another 12 h and cooled to room temperature at the rate of 2 K $min^{-1}$. The structure of the sample was analyzed by x-ray diffraction (XRD) using Cu K$\alpha$ radiation at room temperature. The symmetry and the lattice constants were determined by Rietveld analysis of the XRD data using the FULLPROF program [16]. The resistance as a function of temperature was measured by the standard four probe method from 90 to 300 K. The magnetic susceptibility measurements were performed on a Quantum Design superconducting quantum interference device (SQUID) from 4 to 300 K. The current–voltage ($I$–$V$) measurements were made using a Keithley source meter (Model 2400). Silver was deposited on opposite sides of a bar shaped pellet by a vacuum coating unit. Then ohmic contacts were made using silver epoxy (a simple capacitor-like structure). The contact resistance and influence of the measuring leads have been meticulously monitored; they are indeed negligible as found from our measurements.

## 3. Results and discussion

The single-phase character of the electron-doped sample $Ca_{0.85}La_{0.15}MnO_3$ was confirmed by XRD at room temperature. The XRD pattern of the sample was well categorized by an orthorhombic structure with space group $Pnma$. Figure 1 shows experimental and calculated XRD patterns for the sample. The obtained structural parameters listed in table 1 show that one of the Mn–O(2) bonds (1.973 Å) is much larger than the other Mn–O(2) (1.945 Å) and the Mn–O(1) (1.939 Å) bond. This produces internal distortion in the Mn–O octahedra without changing the symmetry ($Pnma$), but modifies the crystal structure in such a way that $(b/\sqrt{2}) < a < c$ (O′-$Pnma$) [17]. The small Mn–O–Mn angles also bear significance. The

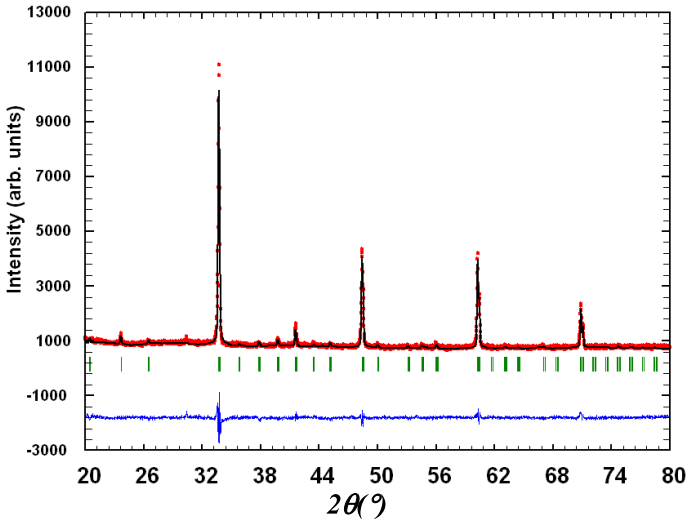


**Figure 1.** The XRD patterns of $Ca_{0.85}La_{0.15}MnO_3$. The dots represent the experimental data and the calculated value is the continuous line overlapping them. The lowest curve shows the difference between the experimental and calculated patterns. The vertical bars indicate Bragg's reflection positions.

**Table 1.** Refined structural parameters (at 300 K) (O(1) and O(2) denote the apical oxygen and basal plane oxygen, respectively. Brackets beside the numerals denote the standard deviation of the last digit.): activation energy derived from equations (1) and (2) (as discussed in the text) and hopping distance from equation (2) for the $Ca_{0.85}La_{0.15}MnO_3$ sample.

| Structure | Orthorhombic |
|---|---|
| Space group | *Pnma* |
| $a, b, c$ (Å) | 5.318 70(6), 7.513 25(7), 5.313 14(5), |
| $V$ (Å$^3$) | 212.317 |
| Mn–O(1)–Mn (deg.), Mn–O(2)–Mn (deg.) | 151.24(9), 159.66(5) |
| Mn–O(1) (Å); Mn–O(2) (Å) | 1.939(3); 1.973(7), 1.945(1) |
| $E_p$ (meV) from resistivity fit (equation (1)) | 21.68 (between 160 and 300 K)<br>238.63 (between 90 and 150 K) |
| $E_p$ (meV) from $I$–$V$ fit (equation (2)) | 11.21 (at 200 K)<br>216.54 (at 100 K) |
| $\xi$ (Å) from $I$–$V$ fit (equation (2)) | 4.57 (at 200 K)<br>5.41 (at 100 K) |

small values reduce the electronic bandwidth and are also associated with many interesting features of the magnetic and transport properties of this compound.

As illustrated by the resistivity curve in figure 2, $Ca_{0.85}La_{0.15}MnO_3$ remains insulating in the entire measured temperature range (90–300 K). The sudden increase in the resistivity curve at ≈150 K suggests appearance of the charge ordered (CO) transition below this temperature. The CO transition is also vividly depicted by the peak in the customary $\mathrm{d}\ln\rho/\mathrm{d}(1/kT)$ versus $T$ plot (inset of figure 2). However, the large gap of about 250 meV appears just at the CO transition, which indicates a very large energy associated with the CO process. Magnetic measurements of this system reveal a antiferromagnetic Néel temperature $T_N$ at ≈160 K (figure 3). Moreover, clear irreversibility between the field cooled (FC) and zero field cooled (ZFC) magnetization values below the CO temperature is also quite significant. The observed

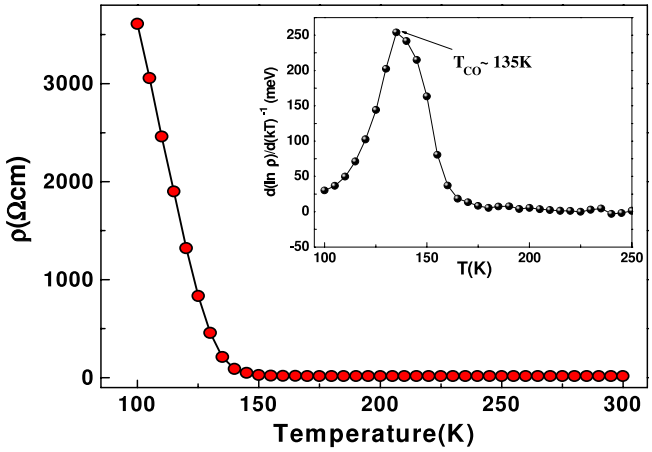


**Figure 2.** Thermal variation of the resistivity of $Ca_{0.85}La_{0.15}MnO_3$. The inset shows the $d(\ln \rho)/d(1/kT)$ versus $T$ plot. A peak corresponding to a large energy gap is observed depicting the $T_{CO}$.

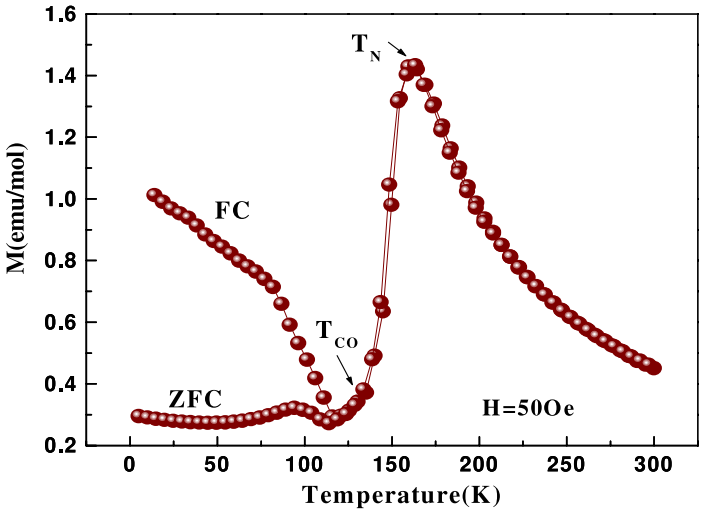


**Figure 3.** Thermal behavior of zero field cooled (ZFC) and field cooled (FC) magnetization for $Ca_{0.85}La_{0.15}MnO_3$ showing pronounced difference in FC and ZFC values.

hysteresis in the FC–ZFC magnetization, below $T_{CO}$, reflects competition between AF coupled $t_{2g}$ and the incipient FM coupled $e_g$ states causing magnetic frustration. The existence of such a magnetically frustrated state has been explained on the basis of phase separation in the case of the PrCaMnO system [18].

In the paramagnetic state, the small polaron hopping conduction mechanism in the adiabatic limit has been reported by several authors [19]. The expression for the electrical resistivity following polaron hopping conduction can be written as

$$\rho = \rho_0 T \exp(E_p/k_B T), \tag{1}$$

where $\rho_0$ is a constant and $E_p$ is the total activation energy of a polaron. The experimental resistivity data was found to be well fitted with equation (1) (as shown in figure 4) in two

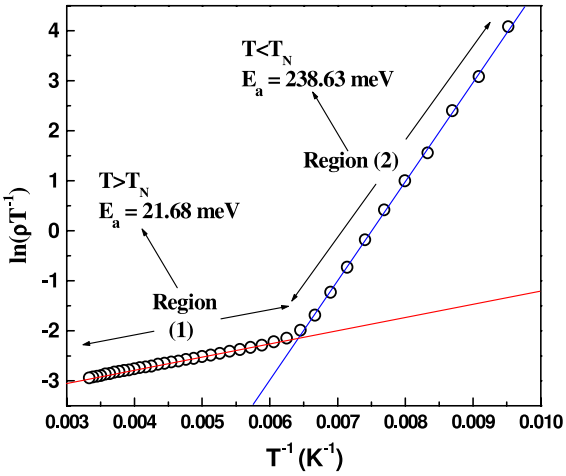


**Figure 4.** The $\ln(\rho/T)$ versus $1/T$ plot for the $Ca_{0.85}La_{0.15}MnO_3$ sample. Straight lines represent fitting results according to equation (1) in two different temperature zones, namely 90–150 K and 160–300 K.

different temperature zones (90–150 K and 160–300 K), generating two values of $E_p \approx 21.68$ meV at $T \geqslant 160$ K (i.e. above $T_N$) and $E_p \approx 238.63$ meV below $T_N$ till 90 K. It is to be noted here that the activation energy increases manifold in the antiferromagnetic charge ordered state in comparison to that of the paramagnetic phase. Such a change in the hopping activation energy is related to the temperature dependent fluctuations of the magnetic semiconductor [20]. In particular, the small polaron motion in a ferromagnetic system is only weakly dependent on the magnetic order; it changes little as the temperature is raised above the Curie temperature. However, in an antiferromagnetic system, the fact that the internal magnetic field changes sign between different sub-lattices gives rise to a significant effect. Namely, below the Néel temperature, there is a change in the average magnetic environment experienced by a carrier (small polaron in the present case) as it hops between different sub-lattices. Therefore, below the Néel temperature the activation energy of the small polaron is augmented by an amount of the order of $\approx k_B T_N$ [21]. In order to confirm this assumption, we have fitted the resistivity data (figure 5) of $CaMnO_3$, which[2] exhibit a paramagnetic to antiferromagnetic transition at 125 K. It is found that in the PM phase $E_p \approx 42.18$ meV and in the AFM region the corresponding value is 52.31 meV; the difference is about 10.13 meV, which is in close agreement with the $k_B T_N$ value (=10.77 meV).

But in case of $Ca_{0.85}La_{0.15}MnO_3$ in the antiferromagnetic phase, this difference between the experimental value (238.63 meV) and the theoretical value ($\approx k_B T_N = 13.78$ meV) is found to be quite high ($\sim$224.85 meV). In order to explain this anomaly, it is necessary to invoke the charge ordered scenario in the present discussion. The large increase in the activation energy actually occurs due to the regular alignment of carriers in the charge ordered state.

The above contention can be proved from the study of the current–voltage ($I$–$V$) characteristic in the temperature range 90–300 K. As seen from figure 6, the $I$–$V$ curve is linear at room temperature. But non-linearity appears below the CO transition temperature. This non-linearity persists till the lowest measurement temperature (90 K) is attained. The non-linearity of $I$–$V$ curves, observed for $T < T_{CO}$, can be explained by considering a percolation process

[2] $CaMnO_3$ was synthesized by the solid state reaction technique, the resistivity was measured using the four probe method and magnetic measurements were made using a SQUID.

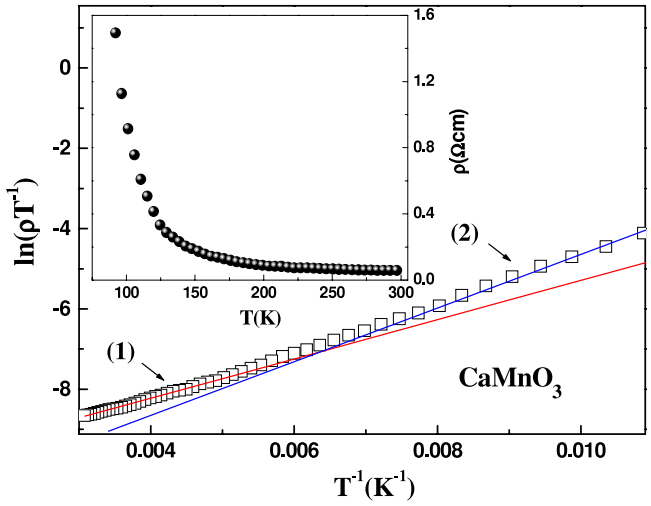


**Figure 5.** The $\ln(\rho/T)$ versus $1/T$ plot for $CaMnO_3$. Straight lines represent fitting results according to equation (1) in two different temperature zones above and below the Néel temperature. The inset shows the thermal variation of resistivity of $CaMnO_3$.

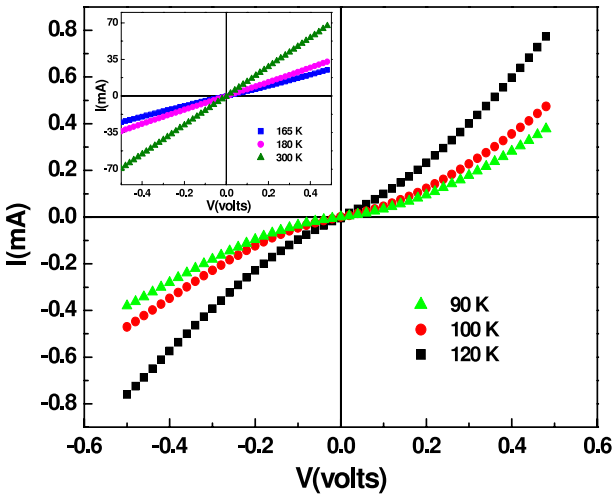


**Figure 6.** The $I$–$V$ characteristic curves measured at different temperatures for the sample $Ca_{0.85}La_{0.15}MnO_3$. The inset shows the same data measured at higher temperatures.

due to melting of the CO insulating phase to the metallic one. This interpretation is based on the opening of metallic-filament paths in a CO insulator matrix [22].

Small polaron hopping character has also been supported from the $I$–$V$ characteristics [23], which can be represented in the form

$$I \propto \sinh(e\xi V/2k_{\mathrm{B}}Td)\exp(-E_{\mathrm{p}}/k_{\mathrm{B}}T) \tag{2}$$

where $\xi$ is the hopping distance, $d$ is the distance between the two electrodes generating the electric field and $E_{\mathrm{p}}$ is the activation energy. We have successfully fitted the experimental $I$–$V$ curves with equation (2), as shown in figure 7. The values of the activation energy of the carriers $E_{\mathrm{p}}$ and hopping distance $\xi$ at various temperatures have been deduced from the

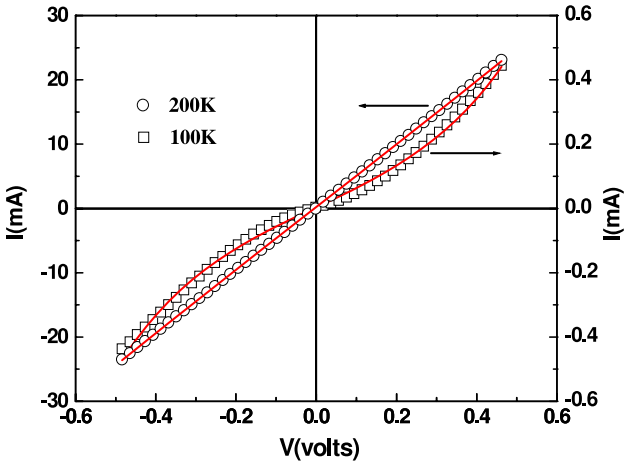


**Figure 7.** The $I$–$V$ curves of the sample $Ca_{0.85}La_{0.15}MnO_3$ fitted with equation (2) at two different temperatures 100 and 200 K.

fitting parameters (shown in table 1). Thus the $I$–$V$ data also justify the small polaron hopping conduction mechanism both in paramagnetic and antiferromagnetic phases in the electron-doped system $Ca_{0.85}La_{0.15}MnO_3$ of the present investigation.

## 4. Summary and conclusion

In summary, the conduction mechanism of the electron-doped charge ordered $Ca_{0.85}La_{0.15}MnO_3$ system obeys the small polaron hopping model throughout the paramagnetic high temperature (160–300 K) and antiferromagnetic low temperature (90–150 K) phases. The activation energy is manifold higher in the low temperature antiferromagnetic region as compared to the corresponding high temperature value in the paramagnetic region. This higher value is attributed to the antiferromagnetic phase as well as to the charge ordering phenomenon. Moreover, the splitting in ZFC–FC magnetization curves below $T_{CO}$ indicates magnetic frustration in this compound appearing as a consequence of random competing interactions, namely, the ferromagnetic double-exchange and the antiferromagnetic super-exchange interactions, in particular due to the possible presence of phase separation, which encourages further studies.

## References

[1] Von Helmolt R, Wecker J, Holzapfel B, Schultz L and Samwer K 1993 *Phys. Rev. Lett.* **71** 2331
[2] Zener C 1951 *Phys. Rev.* **82** 403
[3] Millis A J, Littlewood P B and Shraiman B I 1995 *Phys. Rev. Lett.* **74** 5144
[4] Jin S, Tiefel T H, McCormack M, Fastnact R A, Ramesh R and Chen L H 1994 *Science* **264** 413
[5] Ju H L, Kwon C, Li Q, Greence R L and Venkatesan T 1994 *Appl. Phys. Lett.* **65** 2108
[6] Manoharan S S, Vasanthachaya N Y, Hegde M S, Satyalakshmi K M, Prasad V and Subramanyam S V 1994 *J. Appl. Phys.* **76** 3923
[7] Xiong G C, Li Q, Ju H L, Greence R L and Venkatesan T 1995 *Appl. Phys. Lett.* **66** 1689
[8] Singh S K, Palmer S B, Mck Paul D and Lees M R 1996 *Appl. Phys. Lett.* **69** 263
[9] Bao W, Axe J D, Chen C H and Cheong S W 1997 *Phys. Rev. Lett.* **78** 543
[10] Murakami Y, Shindo D, Chiba H, Kikuchi M and Syono Y 1997 *Phys. Rev.* B **55** 15043
[11] Wollan E O and Koehler W C 1955 *Phys. Rev.* **100** 545
[12] Chiba H, Kikuchi M, Kusaba K and Syono Y 1996 *Solid State Commun.* **99** 499

[13] Troyanchuk I O, Samsonenko N V, Szymczak H and Nabialek 1997 *J. Solid State Chem.* **131** 144
[14] Maignan A, Martin C, Damay F and Raveau B 1998 *Chem. Mater.* **10** 950
[15] van Roosmalen J A M and Cordfunke E H P 1994 *J. Solid State Chem.* **110** 109
[16] Rodriguez Carvajal J 1992 *Physica* B **192** 55
[17] Rivadulla F, López-Quintela M A, Hueso L E, Jardón C, Fondado A, Rivas J, Causa M T and Sánchez R D 1999 *Solid State Commun.* **110** 179
[18] Cox D E, Radaelli P G, Marezio M and Cheong S-W 1998 *Phys. Rev.* B **57** 3305
[19] Pal S, Bose E, Chaudhuri B K, Yang H D, Neeleshwar S and Chen Y Y 2005 *J. Magn. Magn. Mater.* **293** 872
Zhao J H, Kunkel H P, Zhou X Z and Williams G 2001 *J. Phys.: Condens. Matter* **13** 9349
Worledge D C, Miéville L and Geballe T H 1993 *J. Appl. Phys.* **83** 5913
[20] Keem J E, Honig J M and Van Zandt L L 1978 *Phil. Mag.* B **37** 537
[21] Emin D and Liu N L H 1983 *Phys. Rev.* B **27** 4788
[22] Guha A, Raychaudhuri A K, Raju A R and Rao C N R 2000 *Phys. Rev.* B **62** 5320
Asamitsu A, Tomioka Y, Kuwahara H and Tokura Y 1997 *Nature* **388** 50
[23] Böttger H and Bryksin V V 1985 *Hopping Conduction in Solids* (Berlin: Akademie)